

Surface States and the Photoelectron-Spin Polarization of Ni(100)

J. L. Erskine

Department of Physics, University of Texas, Austin, Texas 78712

(Received 5 June 1980)

High-resolution angle-resolved photoelectron emission spectra for Ni(100) are reported which identify a magnetic surface state just below the Fermi level. This surface state exists throughout the surface Brillouin zone including the zone-center $\bar{\Gamma}$ where its room-temperature binding energy and intrinsic width are 0.11 and 0.15 eV, respectively. These new results provide additional insight into the long-standing electron-spin polarization-sign-reversal controversy.

PACS numbers: 79.60.Cn, 73.20.Cw, 75.25.+z

Spin-polarized photoelectron emission studies of single-crystal Ni surfaces reported by Eib and Alvarado¹ have stimulated considerable interest recently. The most striking experimental feature for the (100) Ni surface is the abrupt sign reversal of measured electron-spin polarization (ESP) at approximately 0.1 eV above emission threshold. This result has direct bearing on several important issues related to the inability of one-electron band theory to account for the valence spectra of Ni. Several explanations for the abrupt sign change have been proposed based on distinctly different mechanisms, and at present, the issues are not completely resolved.

Smith and Chiang² have considered the polarization sign reversal within the framework of a three-step model and conclude that a surface-derived photoemission process is needed to explain the observed behavior near threshold. Two distinct surface processes have been proposed. One model, proposed by Moore and Pendry,³ involves a rigorous photoemission calculation which includes photoemission via evanescent low-energy electron-diffraction (LEED) states resulting from the surface potential. This calculation utilizes a bulk band model for Ni having a Stoner gap of about 0.1 eV at the X point as deduced from photoemissions data by Himpsel, Knapp, and Eastman.⁴ A second model, proposed by Dempsey and Kleinman,⁵ is based on emission from a majority-spin surface state which is found just below the Fermi energy in parametrized calculations of the energy bands for a 35-layer (100) Ni crystal.

Moore and Pendry's explanation requires an X_5 exchange splitting of approximately 0.33 eV, a value considerably smaller than 0.88 eV obtained by Wang and Callaway⁶ based on one-electron band theory. As discussed by Liebsch,⁷ the reduced exchange splitting along with the experimentally observed band narrowing, the large

quasiparticle damping and shakeup satellites associated with Ni band spectra can all be understood semiquantitatively based on correlation effects involving $3d$ electrons. Kleinman⁸ has also shown that correlation effects can reduce the X_5 exchange splitting and account for band narrowing, but maintains that a majority-spin surface state accounts for the ESP sign reversal.

Plummer and Eberhardt⁹ have used angle-resolved photoelectron emission to probe for surface states on the (100) surface of nickel. They found a narrow surface sensitive peak near the Fermi energy which could be clearly identified as a surface state in regions of the surface Brillouin zone approaching the zone edge in both the $[10]$ and $[11]$ directions. The peaks become increasingly difficult to characterize as surface states near the center of the two-dimensional zone because of competing emission features. By projecting the bulk bands onto the surface Brillouin zone, they demonstrated that the observed states are magnetic, but it was not possible to relate these surface states directly to the ESP sign reversal because near emission threshold, the most important region of the surface Brillouin zone is centered around $\bar{\Gamma}$, the zone center.

This paper reports results of experiments based on suggestions by Plummer and Eberhardt⁹ which more clearly indicate the extent that surface states are related to the ESP sign reversal: very high-resolution measurements to determine the actual binding energy and intrinsic width of the surface states, and temperature-dependent studies to probe for exchange effects associated with the surface states. In conducting these experiments, it was possible to show that a feature characteristic of surface states exists at $\bar{\Gamma}$ in the surface Brillouin zone. This new result supports the theoretical predictions of Dempsey and Kleinman⁵ and provides an alternate explanation for the long-standing sign reversal controversy based

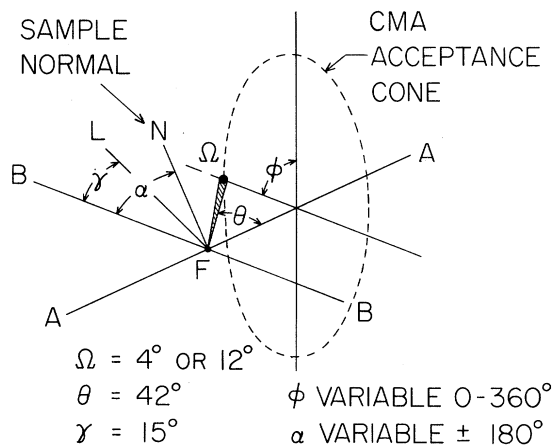


FIG. 1. Experimental geometry: points A , B , L , N , and F are in the same plane; \overline{AA} , CMA axis; F , target point; \overline{LF} , axis of incident photons; \overline{NF} axis of sample normal; emission angle $\theta_e = \pi/2 - \theta - \alpha$.

on direct experimental results.

The experiments reported here were conducted using a high-intensity resonance lamp based on a design reported by Shevchik¹⁰ and a Physical Electronics twin-pass cylindrical-mirror analyzer (CMA) equipped with an angle-resolving drum and a coaxial electron gun for Auger analysis. The sample geometry, shown in Fig. 1, permits sweeping crystal-momentum space along a symmetry direction by either rotating the crystal in the plane of light incidence (angle α) or by rotating both the crystal and the CMA drum (angles α and ϕ). In the experiments reported here, a 4° angle resolving aperture (angle Ω) was used and the angles of incidence $\theta_i = (\alpha - \gamma)$ correspond to predominately s -polarized light.¹¹

The nickel crystal was spark cut and aligned to approximately $\pm 1^\circ$ with use of x-ray Laue techniques, and the orientation of the crystal in the sample mount was checked with use of the same method. Standard cleaning techniques involving argon-ion sputtering, annealing in oxygen, and flashing to high temperatures were used to clean the crystal. Auger analysis was used to ensure that the surface was clean or had only the desired adsorbate impurities. Sulphur and oxygen were adsorbed on the surface (by admitting H_2S or O_2) to test the sensitivity of the surface-state features to chemisorbed layers.

Figure 2 shows high-resolution photoelectron spectra for the (100) crystal face of nickel for values of k_{\parallel} around $\bar{\Gamma}$. Here k_{\parallel} is given by $k_{\parallel} = [(2m/\hbar^2)E_{\text{kin}}]^{1/2} \sin \theta_e$, where E_{kin} is the electron kinetic energy and θ_e is the emission angle

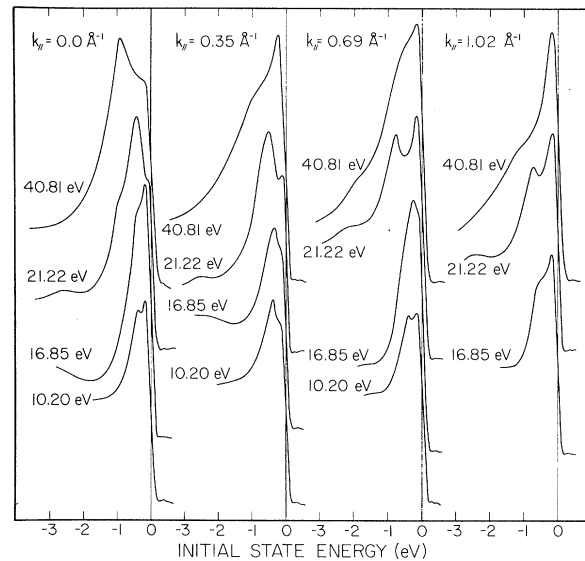


FIG. 2. Angle-resolved photoelectron spectra near the $\bar{\Gamma}$ point of a nickel (100) surface. The k_{\parallel} values correspond to the $\bar{\Gamma}-\bar{M}$ direction. Resolution: $70 \text{ meV} \times 3\%$; selected energy distribution curves were taken at 40-meV resolution. Incident light is predominately s polarized.

measured from the normal. A common feature of these spectra is a narrow peak (or shoulder in some cases) near the Fermi level. This feature satisfies the conditions for a surface state: (i) The binding energy at fixed k_{\parallel} exhibits no dispersion as the perpendicular component of \vec{k} is changed, (ii) analogous spectra (same k_{\parallel} and $\hbar\omega$) after exposure to O_2 and H_2S show that the peak near E_F has higher sensitivity to chemisorption than other features of the spectra, (iii) the binding energy of the peak puts it in an absolute gap of the majority-spin bulk band structure as shown in Fig. 6 of Ref. 9.

Allowed bulk transitions are $\Delta_1 \rightarrow \Delta_1$ and $\Delta_1 \rightarrow \Delta_5$. The predicted surface state couples to s -polarized light, and Δ_1 transitions are forbidden for s polarization. The experimental data exhibit increased emission strength of the feature attributed to a surface state as s polarization is increased.¹¹ The opposite would be expected if the peak were due to Δ_1 transitions. Also, both Δ_1 and Δ_5 bulk transitions should yield observable dispersion at fixed k_{\parallel} . The only reasonable conclusion is the peak near E_F is due to a magnetic surface state.

The binding energy and intrinsic width of the peak near E_F were determined by measuring energy distribution curves at successively higher

analyzer resolution (by decreasing the pass energy of the analyzer). The actual resolution was judged from the sharpness of the Fermi edge, but a "theoretical" resolution of approximately 40 meV was achieved with use of the 10.20-, 16.85-, and 21.22-eV lines, and 100 meV with use of the 40.81-eV line.¹² To obtain the actual width and binding energy near $\bar{\Gamma}$, the 21.22-eV spectra at $k_{\parallel} = 0$ and $k_{\parallel} = 0.35 \text{ \AA}^{-1}$ were analyzed with use of a curve-fitting routine which optimized the fit of a double Gaussian function

$$Y(E) = C_1 \exp[-(E - \mu_1)^2 / 2\sigma_1^2] + C_2 \exp[-(E - \mu_2)^2 / 2\sigma_2^2]$$

to the experimental data. No background contribution is included in the fit, and no correction for the Fermi function was used in fitting the room-temperature data. This was justified based on nearly identical experimental results obtained at 60°K (see Fig. 3). Note also that the shoulder in the 21-eV $k_{\parallel} = 0$ spectra is outside the selected energy range used in modeling. Neglecting this structure introduces negligible error in placing the center and width of the peak near E_F .

The parameters given in Table I establish the binding energy μ_2 and intrinsic width full width at half maximum (FWHM) $= 2\sigma_2(2 \ln 2)^{1/2}$ of the structure at $\bar{\Gamma}$: $\mu_2 = -0.11 \text{ eV}$ and FWHM $= 0.146 \text{ eV}$. These parameters are compatible with the trend apparent in Fig. 7 of Plummer and Eberhardt's paper which illustrates intrinsic width versus binding energy for other surface states identified on metal surfaces. The experimental data (Fig. 2) suggest that the structure disperses downward from E_F away from $\bar{\Gamma}$, and at $k_{\parallel} = 1.02 \text{ \AA}^{-1}$ has a binding energy of 0.14 eV.

The temperature dependence of the structure near E_F was studied in order to observe the influence of exchange effects. During these experiments, the temperature was measured by a Chromel-Alumel thermocouple spotwelded to the back of the sample. Heating pulses were applied at 60 Hz at a duty cycle of less than $\frac{1}{2}$. During the heating part of a cycle, the counting electronics

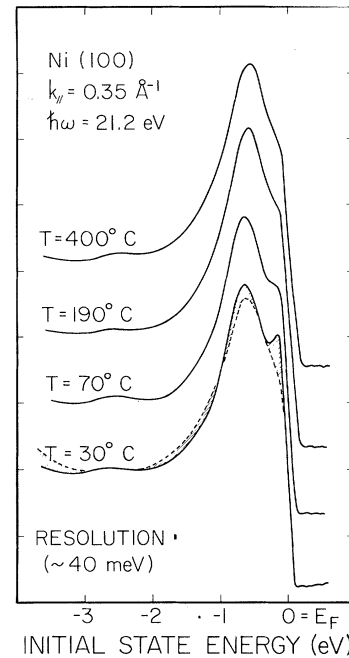


FIG. 3. Temperature dependence of the photoelectron spectra at $k_{\parallel} = 0.35 \text{ \AA}^{-1}$ taken at 21.2-eV photon energy. Resolution: 40 meV \times 2%. Data taken at low temperature (60°K) was nearly identical to the 30°K spectra. Shaded region of lower curve illustrates typical effect of sulfur or oxygen chemisorption ($\sim 1 \text{ L}$). (1 langmuir = 1 L = 1 μ Torr sec.)

were gated off to avoid measuring any influence of the magnetic field on electron trajectories. The sample could also be cooled to below 60°K.

Figure 3 illustrates the temperature dependence near $\bar{\Gamma}$. Data obtained at 60°K matched room-temperature results as stated before. At higher temperatures clear evidence of temperature broadening of the Fermi level appears in the experimental data. Computer modeling with use of the double Gaussian function indicates that the emission from the peak at E_F is reduced relative to the peak at 0.6 eV. Taking into account the Fermi function, it was determined that this decrease in amplitude is accompanied by a small shift of the peak toward the Fermi energy. Auger

TABLE I. Parameters for the double Gaussian function (see text) which yield a best fit to room-temperature experimental data at $h\omega = 21.2 \text{ eV}$.

	C_1	C_2	μ_1 (eV)	μ_2 (eV)	σ_1 (eV)	σ_2 (eV)
$k_{\parallel} = 0$	0.958	0.120	-0.512	-0.112	0.390	0.062
$k_{\parallel} = 0.35 \text{ \AA}^{-1}$	0.997	0.275	-0.536	-0.102	0.410	0.095

analysis was used to show that the effects are not due to sulfur or carbon diffusing to the surface. Also, the process is reversible; room-temperature data is repeated when the sample cools to room temperature.

Presumably, the surface-state binding energy decreases with increasing temperature permitting electrons to spill out of this state and thus reducing its emission amplitude. The fact that an observable shoulder remains at 400 °C (above the Curie temperature) indicates that the temperature-dependent shift in binding energy for this surface state is less than its binding energy, but clearly not zero.

In summary, this paper reports a previously unobserved feature in the Ni(100) photoemission spectra. Within experimental limits this feature satisfies all conditions for a surface state, and it is identified as resulting from a *magnetic* surface state near $\bar{\Gamma}$. This new result places important constraints on the interpretation of ESP experiments in terms of bulk band structure.

It is a pleasure to acknowledge many helpful discussions with L. Kleinman, and support from the Research Corporation, and the National Science Foundation under Grant No. DMR-79-23629.

¹W. Eib and F. S. Alvarado, Phys. Rev. Lett. **37**,

444 (1976).

²N. V. Smith and S. Chiang, Phys. Rev. B **10**, 5013 (1979).

³I. D. Moore and J. B. Pendry, J. Phys. C **11**, 4615 (1978).

⁴F. J. Himpsel, J. A. Knapp, and D. E. Eastman, Phys. Rev. B **19**, 2919 (1979).

⁵D. G. Dempsey and L. Kleinman, Phys. Rev. Lett. **39**, 1297 (1977); D. G. Dempsey, W. R. Grise, and L. Kleinman, Phys. Rev. B **18**, 1270 (1978).

⁶C. S. Wang and J. Callaway, Phys. Rev. B **15**, 298 (1977).

⁷A. Liebsch, Phys. Rev. Lett. **43**, 1431 (1979).

⁸L. Kleinman, Phys. Rev. B **19**, 1295 (1979).

⁹E. W. Plummer and W. Eberhardt, Phys. Rev. B **20**, 1444 (1979).

¹⁰N. Shevchik, J. Electron Spectrosc. **14**, 411 (1978).

¹¹The resonance lamp radiation was not polarized.

At $\hbar\omega = 21.2$ eV, incident angles corresponding to $k_{\parallel} = 0.0 \text{ \AA}^{-1}$, 0.35 \AA^{-1} , and 0.69 \AA^{-1} were 33° , 23° , and 3° which produce incident "p" components of approximately 27%, 20%, and 2% of the total field.

¹²Resolution in the retardation mode is given by $0.007E_p$ (small aperture) or $0.02E_p$ (large aperture), where E_p = pass energy of the analyzer. Based on source size and pass-energy settings, selected spectra were obtained using an estimated resolution of approximately 40 meV. These spectra did not differ from spectra taken with use of an estimated resolution of approximately 60 meV. At values of resolution worse than 100 meV the Fermi edge smears out and the resolved peak at E_F becomes a shoulder (at what appears to be a higher binding energy; see Ref. 9).

Observation of the Meissner Effect in an Organic Superconductor

K. Andres, F. Wudl, D. B. McWhan, G. A. Thomas, D. Nalewajek, and A. L. Stevens

Bell Laboratories, Murray Hill, New Jersey 07974

(Received 5 September 1980)

A partial Meissner effect, fully diamagnetic shielding signals, and large anisotropies in the upper and lower critical fields in ditetramethyltetraselenafulvalene-hexafluorophosphate [(TMTSF)₂PF₆] under applied hydrostatic pressure are observed.

PACS numbers: 74.30.Ci, 72.80.Le, 74.70.Rv

The compound ditetramethyltetraselenafulvalene-hexafluorophosphate [(TMTSF)₂PF₆] is a highly conducting linear-chain organic crystal. At atmospheric pressure, Bechgaard *et al.*¹ have observed a conductivity $\sigma \approx 10^5 (\Omega \text{ cm})^{-1}$ near a temperature of 20 K. Below about 15 K the material enters a semiconducting state which resembles the Peierls state observed in a number of similar compounds.² At a hydrostatic pressure $P = 1.2$ GPa, Jerome *et al.*³ have found that the semiconducting transition is absent and that there

is a new transition at 0.9 K where σ increases by over 10^5 . With the application of magnetic fields of order 200 Oe, the transition temperature T_c drops, and the magnitude of the rise in σ decreases to ~ 5 . Subsequent ac susceptibility measurements⁴ at a frequency $\nu = 68$ Hz show an anomaly indicative of a transition into a diamagnetic state. Jerome *et al.*³ have suggested that (TMTSF)₂PF₆ at $P = 1.2$ GPa is a BCS superconductor.⁵

Although there have been several theoretical models for high conductivity in one-dimensional